

# High Field behavior of the Spin Gap compound $\text{Sr}_2\text{Cu}(\text{BO}_3)_2$

Suchitra E. Sebastian<sup>1</sup>, D. Yin<sup>1</sup>, P. Tanedo<sup>1</sup>, G. A. Jorge<sup>1</sup>, N. Harrison<sup>2</sup>, M.

Jaime<sup>2</sup>, Y. Mozharivskyj<sup>3</sup>, G. Miller<sup>3</sup>, J. Krzystek<sup>4</sup>, S. A. Zvyagin<sup>4</sup>, I. R. Fisher<sup>1</sup>

<sup>1</sup>*Geballe Laboratory for Advanced Materials and Department of Applied Physics, Stanford University, Stanford, CA 94305*

<sup>2</sup>*MST-NHMFL, Los Alamos National Laboratory, Los Alamos, NM 87545*

<sup>3</sup>*Department of Chemistry, Iowa State University, Ames, IA 50011 and*

<sup>4</sup>*National High Magnetic Field Laboratory, Tallahassee, FL 32310*

(Dated: 26th September 2018)

We report magnetization and heat capacity measurements of single crystal samples of the spin gap compound  $\text{Sr}_2\text{Cu}(\text{BO}_3)_2$ . Low-field data show that the material has a singlet ground state comprising dimers with intradimer coupling  $J = 100$  K. High field data reveal the role of weak interdimer coupling. For fields that are large compared to the spin gap, triplet excitations are observed for significantly smaller fields than predicted for isolated dimers, indicating that weak interdimer coupling leads to triplet delocalization. High field magnetization behavior at low temperatures suggests additional cooperative effects.

Recently, the spin gap system  $\text{SrCu}_2(\text{BO}_3)_2$  which is a physical realization of the Shastry-Sutherland model [1], has received a considerable amount of interest [2-5]. Spin frustration in a network of connected dimers leads to competition between Neel and singlet dimer ground states, reducing the spin gap to  $\sim 30$  K. The excited state magnetization is found to be a series of fractional magnetic plateaus of the total magnetization, associated with localized triplet excitations in structures commensurate with the lattice. In this letter, we report results on the first single crystals of the spin gap system  $\text{Sr}_2\text{Cu}(\text{BO}_3)_2$  which although similar in composition to  $\text{SrCu}_2(\text{BO}_3)_2$ , has a very different magnetic lattice and exhibits novel magnetic properties associated with triplet delocalization.

$\text{Sr}_2\text{Cu}(\text{BO}_3)_2$  exists in two structural phases: here we describe the first measurements of single crystal samples of the high temperature  $\beta\text{-Sr}_2\text{Cu}(\text{BO}_3)_2$  phase. This phase is thermodynamically stable above  $\sim 800$  °C, so samples were quenched from 860 °C to room temperature during the growth process.  $\beta\text{-Sr}_2\text{Cu}(\text{BO}_3)_2$  has an orthorhombic unit cell with lattice parameters  $a = 7.612\text{\AA}$ ,  $b = 10.854\text{\AA}$  and  $c = 13.503\text{\AA}$  [6]. The structure is two-dimensional, comprising layers of  $\text{Cu}_2\text{B}_4\text{O}_{12}$  containing  $\text{Cu}^{2+}$  ( $3d^9$ ,  $s = \frac{1}{2}$ ) ions (shown in Figure 1), separated by Sr ions [6]. Each layer comprises distorted octahedral  $\text{Cu}(1)\text{O}_6$  units, square planar  $\text{Cu}(2)\text{O}_4$  units and triangular  $\text{B}(1,2,3)\text{O}_3$  units.

The  $\text{Cu}^{2+}$  ions are coupled via three different exchange pathways (shown as  $J$ ,  $J'$  and  $J''$  in Figure 2) via triangular  $\text{BO}_3$  units. Orthorhombic distortion of the  $\text{Cu}(1)\text{O}_6$  octahedra lifts the  $e_g$  degeneracy of this ion (apical oxygen atoms are further from the central  $\text{Cu}(1)$  atom at  $2.49\text{\AA}$  and  $2.42\text{\AA}$ , than the equatorial oxygen atoms, at  $1.99\text{\AA}$  and  $1.92\text{\AA}$  [6,7]), such that the highest energy level is the antibonding combination of  $\text{Cu } 3d_{x^2-y^2}$  and the equatorial  $\text{O } 2p_\sigma$  orbitals. Since the  $\text{Cu}(1) 3d^9$  hole resides in the equatorial plane, the dominant exchange pathway is therefore  $J$ , through the equatorial oxygen

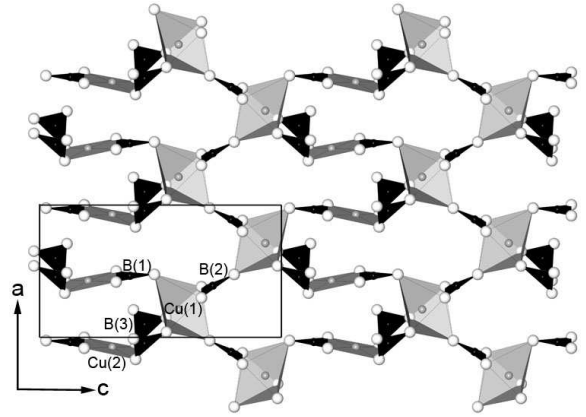


Figure 1:  $\text{Cu}_2\text{B}_4\text{O}_{12}$  layers from  $\beta\text{-Sr}_2\text{Cu}(\text{BO}_3)_2$ . The open circles represent O, the gray circles Cu and the black circles B. Dimer units comprise Cu(1) and Cu(2) atoms linked via B(3) $\text{O}_3$  groups. Sr ions separating the layers are not shown.

ions of the  $\text{Cu}(1)\text{O}_6$  octahedra. The equivalent magnetic lattice (Figure 2a) then comprises  $\text{Cu}(1)\text{-Cu}(2)$  dimers coupled by  $J$  via  $\text{B}(3)\text{O}_3$  triangular units. In this paper, we present high field magnetization measurements that reveal the effect of weak inter-dimer coupling  $J'$  and  $J''$  through  $\text{B}(2)\text{O}_3$  and  $\text{B}(1)\text{O}_3$  groups respectively.

Single crystals of  $\beta\text{-Sr}_2\text{Cu}(\text{BO}_3)_2$  were grown using  $\text{LiBO}_2$  as a flux [6]. The polycrystalline precursor was prepared by a solid state reaction of  $\text{SrCO}_3$ ,  $\text{CuO}$  and  $\text{B}_2\text{O}_3$  ground together in stoichiometric ratios and heated in flowing  $\text{O}_2$  at  $900$  °C for approximately 72 hours with intermediate grindings. A mixture with 1:1.4 molar ratio of polycrystalline  $\text{Sr}_2\text{Cu}(\text{BO}_3)_2$  to  $\text{LiBO}_2$  was heated in a Pt crucible to  $925$  °C, cooled at approximately  $1$  °C per hr to  $860$  °C and the remaining liquid decanted. The crystals were allowed to cool rapidly in air. The resulting single crystals of  $\beta\text{-Sr}_2\text{Cu}(\text{BO}_3)_2$  were multi-faceted, purple in color, with dimensions of up to 5mm on a side.

Magnetization measurements in fields up to 5 T were

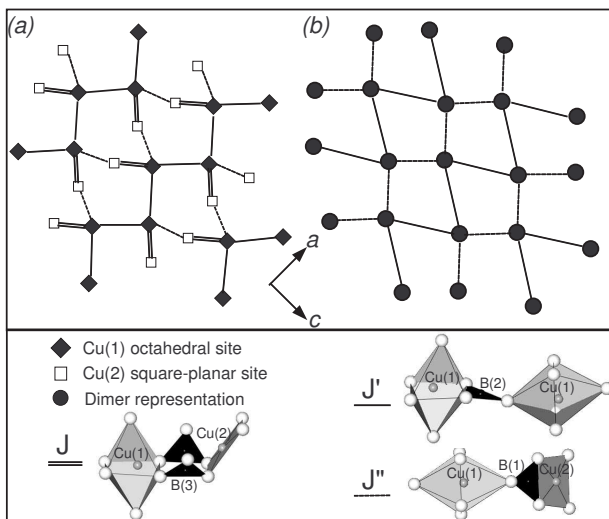


Figure 2: (a) Magnetic lattice representing the structure of  $\text{Cu}_2\text{B}_4\text{O}_{12}$  planes in  $\text{Sr}_2\text{Cu}(\text{BO}_3)_2$ . Atomic positions of  $\text{Cu}(1)$  and  $\text{Cu}(2)$  are taken from the real crystal structure. Exchange pathways are labelled in the legend. (b) In the limit  $J \gg J'$  and  $J''$ , interdimer terms can be treated perturbatively, and the lattice mapped on to a distorted square lattice of dimers. Each dimer unit is represented by a solid circle positioned in the geometric center of the  $\text{Cu}(1)$  and  $\text{Cu}(2)$  atoms.

performed in a Quantum Design SQUID magnetometer. DC magnetic susceptibility ( $\chi = \frac{M}{H}$ ) measured in 5000 Oe with  $H$  aligned along the principal crystal axes is shown in Figure 3. From the exponential behavior at low temperatures, it is clear that the material is a spin gap system. To estimate the intradimer coupling  $J$ , a simple approximation is to fit the magnetic susceptibility to an isolated dimer model with an additional Curie term to account for a small isolated impurity spin concentration:

$$\chi = \frac{N(\mu_B g)^2}{k_B T (3 + \exp(\frac{J}{k_B T}))} + \frac{C}{T} + \chi_0$$

where  $N$  is Avogadro's number,  $C$  the Curie constant due to non-interacting impurities and  $\chi_0$  a temperature-independent term. Any renormalization due to interdimer coupling terms would modify the value of  $g$ . For all three orientations, the magnetic susceptibility per mole of  $\text{Cu}$  spins as a function of temperature can be well fit by the isolated dimer model. The value of  $J$  for all three orientations is found from these fits to be  $100 \pm 1.5$  K in agreement with previous polycrystalline data [7]. Values for  $g$  are found to be  $2.0 \pm 0.05$  for  $H$  aligned along the  $b$  and  $c$ -axes, but  $2.2 \pm 0.05$  for  $H$  aligned along the  $a$ -axis, consistent with the orientation of the  $\text{CuO}_4$  units.  $C$  varies from 0.001 to 0.003  $\text{emuK/molOe}$ , corresponding to 0.3% to 0.8% impurity concentration, assuming impurity spins with  $g = 2$ ,  $s = \frac{1}{2}$ . The  $T$ -independent term  $\chi_0$  is small and positive, likely due to a very small concentration of ferromagnetic impurities. Values vary

slightly between samples and with orientation, and for the data shown in Figure 3 correspond to approximately  $10^{-4} \mu_B$  per formula unit.

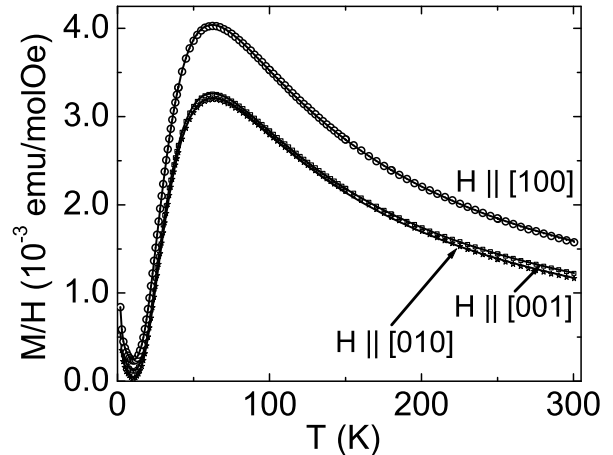


Figure 3: Temperature dependence of the magnetic susceptibility of a single crystal of  $\text{Sr}_2\text{Cu}(\text{BO}_3)_2$  for a field of 5000 Oe aligned along the principal crystal axes. Solid lines show fit to isolated dimer model, described in main text.

Independent measurements of  $g$  are necessary to determine the extent of renormalization of the magnetic susceptibility due to interdimer coupling. Values for  $g$  were obtained via Electron Spin Resonance (ESR) using a Bruker Elexsys E680X spectrometer at X-band frequency 9.38 GHz at room temperature. These measurements gave  $g_a = 2.230$ ,  $g_b = 2.060$  and  $g_c = 2.130 \pm 0.004$  in good agreement with values obtained from susceptibility fits within the uncertainty of these measurements, indicating that any interdimer terms are not large enough to have a measurable effect at low fields.

An additional confirmation of the value of  $J$  in this system is obtained from heat capacity measurements. The Schottky anomaly from the large spin gap is too small to be easily resolved against the large phonon contribution to the heat capacity. However, the shift in heat capacity due to Zeeman splitting of the triplet states in a magnetic field can be observed. Measurements were made in zero field and 18 T continuous field for a single crystal of  $\beta$ - $\text{Sr}_2\text{Cu}(\text{BO}_3)_2$  weighing 7.9 mg. The field was oriented at an arbitrary angle to the crystal. A calorimeter made of plastic materials and silicon was used, employing a thermal relaxation time technique. The difference between these two values,  $\Delta C_p = C_p(18\text{T}) - C_p(0\text{T})$  is due solely to changes in the magnetic contribution and can be calculated for an isolated dimer model using measured values for  $J$  and  $g$  for this crystal. Figure 4 shows calculated and measured values for  $\Delta C_p$  as a function of temperature. The measured data has a broad maximum with a peak value of  $0.38 \pm 0.07$  J/molK centered

at  $14 \pm 1$  K, compared to the model which has a peak value of  $0.32$  J/molK centered at 16 K. The data agree within experimental uncertainty, confirming that the isolated dimer model with  $J = 100$  K is a reasonable first approximation in small magnetic fields.

We note that additional features are evident in the heat capacity at high temperatures (inset to figure 4), which appear to be unrelated to the low temperature magnetic properties. Structural refinements performed on a single crystal indicate no change in symmetry or average atomic positions between the Low Temperature (LT) ( $T < 230$  K), Room Temperature (RT) ( $230$  K  $< T < 320$  K), and High Temperature (HT) ( $T > 320$  K) regions, but a marked change in the thermal parameters of the B atoms indicates a change in vibrational properties.

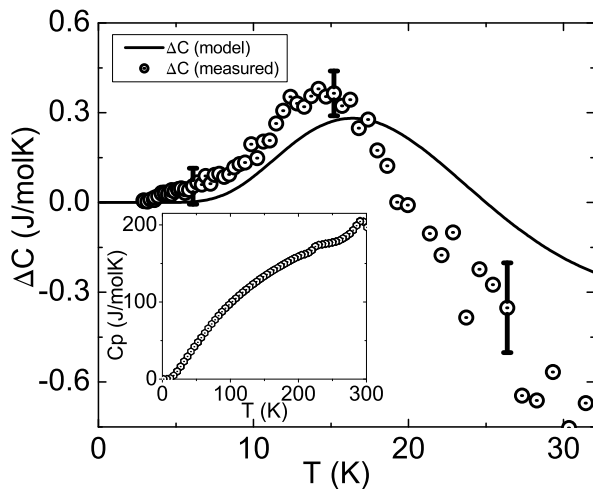


Figure 4: Difference in heat capacity  $\Delta C_p = C_p(18 \text{ T}) - C_p(0 \text{ T})$  for a single crystal of  $\text{Sr}_2\text{Cu}(\text{BO}_3)_2$ . Solid line shows calculated value for dimer model with  $J = 100$  K and  $g = 2.14$ . Inset shows total heat capacity in zero field between 2 K and 300 K. Mol refers to the formula unit.

The behavior of  $\text{Sr}_2\text{Cu}(\text{BO}_3)_2$  is most interesting in high magnetic fields, for which  $g\mu_B H \sim J$ . In particular, we find that the magnetization is no longer fit well by the isolated dimer model, due to the effects of interdimer coupling. Magnetization measurements were made in pulsed high magnetic fields up to 65 T at different temperatures. The data are obtained using a wire-wound sample extraction magnetometer in which the sample is inserted or removed from the detection coils *in situ*. Data were taken for increasing and decreasing fields, and the average value calculated. A collection of six randomly oriented fragments from a clean single crystal was used in order to maximize the filling factor of the coil. Magnetization for this composite sample as a function of field is shown in Figure 5. A small linear diamagnetic contribution with negative slope  $9 \times 10^{-4} \mu_B/\text{T}$ , due to the response of the

source coils, has been subtracted from the data. The value of magnetization at 50 K in a field of 5 T was compared with SQuID magnetometer magnetization data in order to obtain absolute values for the magnetization in units of  $\mu_B/\text{Cu}$ .

A feature of the isolated dimer model is a sharp increase in magnetization to  $1 \mu_B$  when the lowest Zeeman-split triplet state crosses the singlet state at  $T = 0$ . For  $J = 100$  K and  $g = 2.14$  (i.e. average value for the composite sample), this would occur at an applied magnetic field  $H_c = 69$  T if there was no interdimer interaction, with thermal broadening at finite temperatures (solid lines in Figure 5). As shown in Figure 5,  $M(H)$  data correspond very closely to this model for temperatures of 20 K and above, but deviate significantly for lower temperatures. At 1.5 K, data taken to 65 T clearly show the swift rise in magnetization due to triplet excitations. This occurs at a magnetic field lower than  $J$ . Furthermore, data for temperatures of 5 and 10 K coincide with the 1.5 K data within experimental uncertainty.

The deviation from the isolated dimer model is clearly revealed in a graph of magnetization as a function of temperature (Figure 6). In high magnetic fields, the magnetization does not fall to zero at low temperatures, but is as large as  $0.15 \mu_B$  for temperatures below 10 K. Above 15 K, the  $M(T)$  curves rise sharply, coinciding with the isolated dimer model for temperatures above 20 K.

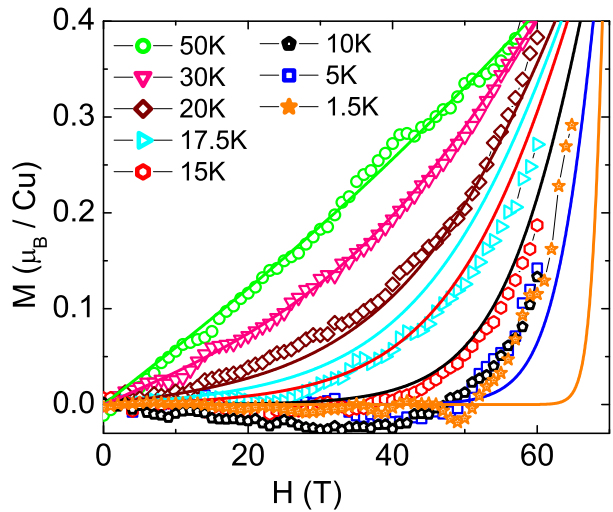


Figure 5: Magnetization of  $\text{Sr}_2\text{Cu}(\text{BO}_3)_2$  as a function of applied field at different temperatures. Calculated values for isolated dimer model with  $J = 100$  K and  $g = 2.14$  shown by solid lines.

The observed high field magnetization behavior at low temperatures indicates that  $\text{Sr}_2\text{Cu}(\text{BO}_3)_2$  is not an isolated dimer system. The upturn in magnetization due to the excitation of singlet into triplet states occurs at

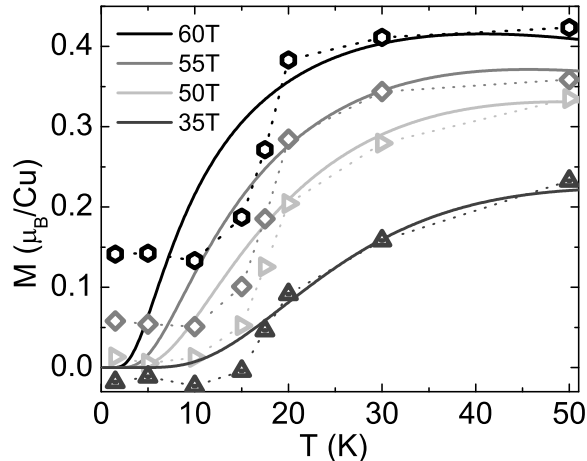


Figure 6: Magnetization as a function of temperature for different magnetic fields. Symbols (connected by dotted lines to guide the eye) indicate measured magnetization data extracted from Figure 5, solid lines indicate isolated dimer model with  $J = 100$  K and  $g = 2.14$

a lower magnetic field  $H_c \sim 56$  T than predicted by the isolated dimer model (67 - 74 T, for  $g$  values between 2.2 and 2.0), indicating that the interdimer exchange terms  $J'$  and  $J''$  have a significant effect. This effect can be estimated if we assume that  $J'$  and  $J''$  are much smaller than  $J$  and can be treated as a perturbation to the isolated dimer model. These interdimer terms act on triplet states and enable triplet hopping from first order in the perturbation solution, resulting in a triplet dispersion relation that reduces  $H_c$  from  $J/g\mu_B$ . This is very different from the Shastry Sutherland compound  $\text{SrCu}_2(\text{BO}_3)_2$ , for which triplets are localized up to the fourth order in the perturbation solution, due to frustration [4]. To obtain an estimate of  $H_c$  in  $\beta\text{-Sr}_2\text{Cu}(\text{BO}_3)_2$ , the simplifying assumption can be made that in the vicinity of level crossing, the eigenspace comprises only the two degenerate singlet ( $S = 0$ ) and lowest triplet ( $S^z = 1$ ) states, which is a reasonable assumption given the large value of  $J$ . These can be mapped on to an effective site which is empty ( $S = 0$ ) or occupied ( $S^z = 1$ ) by a hardcore boson (equivalent to a pseudo-spin  $\frac{1}{2}$ .) The effective sites form a square lattice linked by  $J'$  and  $J''$  (Figure 2b.) Following the perturbative treatment of interdimer terms on a lattice of coupled spin  $\frac{1}{2}$  chains [8,9] we obtain  $g\mu_B H_c = J - \frac{J'+J''}{2}$  for the lattice in Figure 2b. For the observed range  $J/g\mu_B - H_c \simeq 11 - 18$  T (depending on the value of  $g$ ), we obtain  $\frac{J'+J''}{2} \sim 17 - 28$  K. Experiments are in progress to directly measure the triplet dispersion and thereby independently determine the values of  $J'$  and  $J''$ .

At low temperatures and in high magnetic fields, interactions between the triplets will determine the nature of the ground state, which is likely a canted antiferro-

magnet. Within a picture of delocalized triplets, and neglecting anisotropic terms such as Dzyaloshinskii Moriya exchange, it is natural to consider this as a Bose Einstein Condensate of hardcore bosons [9]. The temperature independent finite magnetization below 20 K in high magnetic fields (Figure 6) is presumably associated with this state, following a similar temperature dependence to results from numerical studies of weakly coupled dimer systems [10] and experimental results for the related material  $\text{TlCuCl}_3$  [11,12]. However, only a small portion of the phase diagram is accessible due to the large value of the spin gap, and it is therefore difficult to unambiguously identify the nature of the ground state in high magnetic fields for this material.

In summary, we have made the first magnetization and heat capacity measurements on single crystals of the new spin gap compound  $\beta\text{-Sr}_2\text{Cu}(\text{BO}_3)_2$ . The material has a singlet groundstate comprising dimers with intradimer coupling  $J = 100$  K. High field measurements reveal the presence of interdimer coupling, which results in the reduction of  $H_c$  from  $J/g\mu_B$  and a finite low temperature magnetization at high fields. From these measurements, we estimate weak interdimer coupling  $\frac{J'+J''}{2} \sim 17 - 28$  K. For fields above  $H_c$ , cooperative effects are expected to lead to an ordered ground state, the nature of which remains to be determined.

We acknowledge helpful discussions with C. Batista. This work is supported by the National Science Foundation, Division of Materials Research under DMR-0134613. Experiments performed at the National High Magnetic Field Laboratory were supported by the National Science Foundation through Cooperative Grant No. DMR-9016241 and MRI Grant No. 0079641, the State of Florida, and the Department of Energy. I.R.F acknowledges support from the Alfred P. Sloan Foundation and S.E.S from the Mustard Seed Foundation.

- 
- [1] B. S. Shastry and B. Sutherland, *Physica* **108B**, 1069 (1981).
  - [2] R. W. Smith and D. A. Keszler, *J. Solid State Chem.* **93**, 430 (1991).
  - [3] H. Kageyama *et al.*, *Phys. Rev. Lett.* **82**, 3168 (1999).
  - [4] S. Miyahara and K. Ueda, *Phys. Rev. Lett.* **82**, 3701 (1999).
  - [5] H. Kageyama *et al.*, *J. Phys. Soc. Jpn.* **68**, 1821 (1999).
  - [6] R. W. Smith and D. A. Keszler, *J. Solid State Chem.* **81**, 305 (1989).
  - [7] H. Sakurai *et al.*, *J. Phys. Soc. Jpn.* **71**, 999 (2001).
  - [8] F. Mila, *Eur. Phys. J. B* **6**, 201 (1998).
  - [9] T. Giamarchi and A. M. Tsvelik, *Phys. Rev. B* **59**, 11398 (1999).
  - [10] S. Wessel *et al.*, *Phys. Rev. Lett.* **87**, 206407 (2001).
  - [11] Ch. Rugg *et al.*, *Nature* **423**, 62 (2003).
  - [12] T. Nikuni *et al.*, *Phys. Rev. Lett.* **84**, 5868 (2000).